Journal of Non-Crystalline Solids xxx (2010) xxx–xxx

Contents lists available at ScienceDirect

Journal of Non-Crystalline Solids

journal homepage: www.elsevier.com/ locate/ jnoncrysol

Replica field theory for anharmonic sound attenuation in glasses

C. Tomaras [a,*], B. Schmid [b], W. Schirmacher [b,c]

[a] Arnold Sommerfeld Center for Theoretical Physics, Ludwig-Maximilians-Universität München, Theresienstr. 37, D-80333 München, Germany
[b] Institut für Physik, Universität Mainz, Staudinger Weg 7, D-55099 Mainz, Germany
[c] Physik-Department E13, Technische Universität München, D-85747, Garching, Germany

A R T I C L E I N F O

Article history:
Received 12 April 2010
Received in revised form 14 May 2010
Available online xxxx

Keywords:
Vibrational states in disordered solids;
Phonon–phonon interaction;
Brillouin linewidth

A B S T R A C T

A saddle-point treatment of interacting phonons in a disordered environment is developed. In contrast to crystalline solids, anharmonic attenuation of density fluctuations becomes important in the hydrodynamic regime, due to a broken momentum conservation. The variance of the shear modulus Δ^2 turns out to be the strength of the disorder enhanced phonon–phonon interaction. In the low-frequency regime (below the boson peak frequency) we obtain an Akhiezer-like sound attenuation law $\Gamma \propto T\omega^2$. Together with the usual Rayleigh scattering mechanism this yields a crossover of the Brillouin linewidth from a ω^2 to a ω^4 regime. The crossover frequency ω_c is fully determined by the boson peak frequency and the temperature. For network glasses like SiO_2 at room temperature this crossover is predicted to be situated one order of magnitude below the boson peak frequency.

1. Introduction

Theories for sound-wave propagation in inhomogeneous media (e.g. a spatially fluctuating sound velocity) have served as a common tool for explaining the anomalous vibrational properties of disordered solids for at least two decades [1–12]. However, less is known about the role of the anharmonic interaction in such models. In a previous phenomenological approach, involving only the longitudinal modes, a *Mode-Grüneisen* like 3 phonon interaction has already been incorporated [13]. During the recent years, the detailed vector theory [5], based on Lame's elasticity theory with spatially fluctuating elastic moduli, has gained importance, because it establishes the connection with Raman scattering data [8]. From first principles of elasticity theory, this vector model allows for the inclusion of a phonon–phonon interaction, which depends only on the constants that characterize the harmonic medium, and requires no additional parameters. In the present paper we present the derivation of the generalized anharmonic saddle-point equations within the *replica formalism* [14–16]. We evaluate the anharmonic corrections on the Brillouin linewidth within a perturbative regime. At room temperature the theory predicts anharmonic sound attenuation at the THz scale. This is in agreement with previous simulations [17,18], which report on strong effective Grüneisen parameters, compared with their rather weak crystalline counterparts; in the present treatment the relevant expansion parameter of the anharmonic vertex is just the fluctuation of the shear modulus Δ^2 which typically is of the order $\approx 0.1\rho^2 v_T^4$, whereas the Grüneisen parameters of crystalline solids are much smaller and lead to anharmonic sound attenuation at and below several GHz [19] ($v_{L/T}$ is the longitudinal/transverse sound velocity). Recent experiments [20,21] showed already the existence of anharmonic sound attenuation at the THz scale in SiO_2, e.g. the Brillouin linewidth exhibits an additional ω^2 regime below the disorder-induced Rayleigh ω^4 law, but disagree about the precise value of the crossover frequency separating both regimes. In addition it was widely believed that these anharmonic effects coincided with those of the corresponding crystalline phase, and several authors consulted an old kinetic description of anharmonic solids [22]. However, this kinetic theory only applies to transverse phonons, due to energy and momentum conservation, as we explain in the second section. In contrast, the anharmonic sound attenuation emerging from the present calculation relies crucially on the presence of disorder. The Brillouin linewidth satisfies an Akhiezer-like law, with a prefactor related to the disorder-dressed spectral function. This is more reasonable, because the vibrational degrees of freedom of a glass are assumed to be at thermal equilibrium throughout the whole literature, whereas the kinetic description only applies to non-equilibrium phonon distributions.

2. Theory of anharmonic sound attenuation in glasses

2.1. Anharmonic elasticity

The usual textbook derivation [23,24] of elasticity theory starts with the non-linearized strain tensor,

$$u_{ij}(\mathbf{x},t) = \frac{1}{2}\left(\partial_i \mathbf{u}_j(\mathbf{x},t) + \partial_j \mathbf{u}_i(\mathbf{x},t) + \frac{1}{2}\sum_k \partial_i \mathbf{u}_k(\mathbf{x},t)\partial_j \mathbf{u}_k(\mathbf{x},t)\right) \quad (1)$$

* Corresponding author.
E-mail addresses: constantin.tomaras@physik.uni-muenchen.de, ctomaras@ph.tum.de (C. Tomaras).

0022-3093/$ – see front matter © 2010 Elsevier B.V. All rights reserved.
doi:10.1016/j.jnoncrysol.2010.05.084

which measures the deformation of a differential volume element. The elastic free energy functional $\mathcal{F}_{el}$ to quadratic order

$$\mathcal{F}_{el} = \sum\left(\frac{\lambda}{2}u_{ii}^2 + \mu(\mathbf{x})u_{ij}u_{ij}\right) \tag{2}$$

is built up from the translation and rotational invariant contractions of the strain tensor. If the displacement of the individual atoms from their equilibrium position is small e.g. $\nabla\cdot\mathbf{u}\ll 1$, the non-linear part of Eq. (1) can be neglected. Even then, the residual third order contributions of Eq. (2) and possible third order contractions with independent elastic moduli (Grüneisen-like parameters) have to be taken into account, for explaining other physical properties of solids, likewise a finite thermal conductivity or thermal expansion [25]. As we explain in the next paragraph, the anharmonicities included in Eq. (2) cannot lead to thermalization of the density modes in the crystalline phase.

2.2. Absence of sound attenuation in the hydrodynamic regime

In case of a spatially independent shear modulus $\mu(\mathbf{x}) = \mu_0$ the wave number $\mathbf{k}$ is a good quantum number. According to the continuity equation, longitudinal phonons are density fluctuations $\rho(\mathbf{x},t) = \rho_0\nabla\cdot\mathbf{u}(\mathbf{x},t)$. The absorption of a density wave through an energy and momentum conserving three phonon collision obeys the conservation laws

$$\omega_L + \omega_i^{(1)} = \omega_i^{(2)} \tag{3}$$

$$\mathbf{k}_L + \mathbf{k}_i^{(1)} = \mathbf{k}_i^{(2)}. \tag{4}$$

Applying the triangular inequality to Eq. (4) and inserting Eq. (3) leads to Eq. (6)

$$|\mathbf{k}_L| \geq \left|\mathbf{k}_i^{(2)}\right| - \left|\mathbf{k}_i^{(1)}\right| \tag{5}$$

$$\frac{1}{\upsilon_L} \geq \frac{1}{\upsilon_i}, \tag{6}$$

which states that density fluctuations can only be absorbed by longitudinal phonons. (In a solid $\upsilon_L \geq \upsilon_T$!) In that case Eq. (3) equals

$$|\mathbf{k}_L| + \left|\mathbf{k}_L^{(1)}\right| = \left|\mathbf{k}_L^{(2)}\right|, \tag{7}$$

only collisions with parallel aligned momenta occur. To calculate an extensive decay probability via Fermi's golden rule, the number of possible final states has to be of the order of total degrees of freedom (the number of degrees of freedom is bounded through the Debye cutoff $k_D = \sqrt[3]{6\pi^2 N/V}$). Anharmonic attenuation of density fluctuations would therefore not be observable in the thermodynamic limit ($V\rightarrow\infty$ with finite density), in a translationally invariant system. This series of arguments has been already used by Landau and Rumer in 1936 [26]. In their theory transverse phonons acquire a lifetime due to collisions with thermalized phonons. In 1939 Akhiezer developed the corresponding kinetic theory [22], which takes into account scattering at phonons in a non-equilibrium state. In crystalline solids the Akhiezer regime is reported at frequencies below 1 GHz [19]. Both theories only apply to transverse phonons, and cannot account for high-frequency deviations observed in Brillouin light scattering experiments, which are probing the longitudinal modes.

2.3. Replica field theory

The imaginary time quantum dynamics [27] of the present model emerge from the Euclidean action Eq. (8), in which $u_{ij} = \frac{1}{2}(\partial_i\mathbf{u}_j(\mathbf{x}) + \partial_j\mathbf{u}_i(\mathbf{x}))$ is the linearized strain and $\upsilon_{ij} = \frac{1}{2}(\partial_i\mathbf{u}_j(\mathbf{x}) - \partial_j\mathbf{u}_i(\mathbf{x}))$ the linearized rotation tensor.

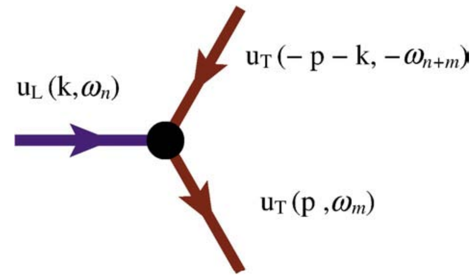

Fig. 1. 3-phonon vertex, the Fourier modes $\mathbf{u}_i(\mathbf{k},\omega_n)$ are defined through Eq. (21).

$$S\left[u_{ij}(\mathbf{x},\tau)\right] = \int_0^\beta d^4x\left(\frac{\rho}{2}u_{ii}\partial_\tau^2 u_{ii} + \frac{\lambda}{2}u_{ii}^2 + \mu(\mathbf{x})u_{ij}u_{ij} + \lambda u_{ii}\upsilon_{ij}\upsilon_{ij} + \mu(\mathbf{x})u_{ij}\upsilon_{il}\upsilon_{lj}\right), \tag{8}$$

Eq. (8) contains an interaction between longitudinal and transverse phonons, for which the perturbation theory can be developed from the elementary vertex shown in Fig. 1.

The probability to absorb or emit a longitudinal phonon vanishes in a translationally invariant model, as the creation of a virtual transverse phonon pair satisfies Eq. (4). However this is not true for a spatially dependent shear modulus, averaging the inverse lifetime $\Gamma[\mu(\mathbf{x})]$ over a certain distribution of $\mu(\mathbf{x})$ yields a finite Brillouin linewidth Γ, as we are averaging strictly positive numbers. Therefore Γ should in general depend only on the local fluctuations $\langle\delta\mu(\mathbf{x})\delta\mu(\mathbf{x})\rangle$, rather than the average $\langle\mu(\mathbf{x})\rangle = \mu_0$, as $\Gamma[\mu_0] = 0$. We assume a Gaussian distribution of the shear modulus $\langle\delta\mu(\mathbf{x})\delta\mu(\mathbf{x}')\rangle = K_\mu(\mathbf{x}-\mathbf{x}')$, and carry out the disorder average applying the replica trick [7,8]. The spatial fluctuations of λ are neglected. This yields the euclidean action in replica space:

$$\begin{aligned} S\left[u_{ij}^a(\mathbf{x},\tau)\right] = &\int_0^\beta d^4x\sum_a\left(\frac{\rho}{2}u_{ii}^a\partial_\tau^2 u_{ii}^a + \frac{\lambda}{2}\left(u_{ii}^a\right)^2 + \lambda u_{ii}^a\upsilon_{ij}^a\upsilon_{ij}^a + \mu_0 u_{ij}^a\upsilon_{il}^a\upsilon_{lj}^a\right) \\ &+ \sum_{ab}\int_0^\beta\frac{d^4x d^4x'}{2\hbar}\left(u_{ij}^a u_{ij}^a(\mathbf{x},\tau)K_\mu(\mathbf{x}-\mathbf{x}')u_{lm}^b u_{lm}^b(\mathbf{x},\tau')\right. \\ &\left.+ u_{ij}^a(\mathbf{x},\tau)\upsilon_{il}^a\upsilon_{lj}^a K_\mu(\mathbf{x}-\mathbf{x}')u_{hk}^b\upsilon_{hm}^b\upsilon_{mk}^b(\mathbf{x}',\tau')\right) \\ &+ \sum_{ab}\int_0^\beta d^4x\int_0^\beta\frac{d^4x'}{\hbar}\left(u_{ij}^a(\mathbf{x},\tau)u_{ij}^a K_\mu(\mathbf{x}-\mathbf{x}')u_{hk}^b\upsilon_{hm}^b\upsilon_{mk}^b(\mathbf{x}',\tau')\right) \end{aligned} \tag{9}$$

We now derive an effective action with the help of the pair modes

$$u_{ij}^a(x)u_{hk}^b(x') = \hbar Q_{ijhk}^{ab}(x,x') \tag{10}$$

$$\upsilon_{ij}^a(x)\upsilon_{hk}^b(x') = \hbar\tilde{Q}_{ijhk}^{ab}(x,x') \tag{11}$$

and their conjugate Lagrange multipliers Λ via the Fadeev–Popov transformation [28]:

$$\begin{aligned} S\left[u_{ij}^a(\mathbf{x},\tau),Q,\tilde{Q}\right] = &\int_0^\beta d^4x\left(\frac{\rho}{2}u_{ii}^a\partial_\tau^2 u_{ii}^a + \frac{\lambda}{2}\left(u_{ii}^a\right)^2 + \lambda u_{ii}^a\tilde{Q}_{ijij}^{aa}(x,x) + \mu_0 u_{ij}^a\tilde{Q}_{illj}^{aa}(x,x)\right) \\ &+ \frac{\hbar^2}{2}\int_0^\beta d^4x'd^4x\left(\frac{K_\mu(\mathbf{x}-\mathbf{x}')}{\hbar}Q_{ijlm}^{ab}(x,x')^2\right. \\ &\left.+ Q_{ijhk}^{ab}(x,x')\tilde{Q}_{ilmk}^{ab}(x,x')K_\mu(\mathbf{x}-\mathbf{x}')\tilde{Q}_{ljhm}^{ab}(x,x')\right) \\ &+ \hbar^2\int_0^\beta d^4x'd^4xQ_{ijkh}^{aa}(x,x)K_\mu(\mathbf{x}-\mathbf{x}')\tilde{Q}_{hmmk}^{bb}(x',x')u_{hk}^b(\mathbf{x}',\tau') + S_{F1} + S_{F2} \end{aligned} \tag{12}$$

Please cite this article as: C. Tomaras, et al., Replica field theory for anharmonic sound attenuation in glasses, J. Non-Cryst. Solids (2010), doi:10.1016/j.jnoncrysol.2010.05.084

$$S_{F1} = \sum_{ijhkab} i\int d^4x \frac{d^4x'}{\hbar} \Lambda^{ab}_{ijhk}(x,x')\left(\hbar Q^{ab}_{ijhk} - u^a_{ij}(x)u^b_{hk}(x')\right) \tag{13}$$

$$S_{F2} = \sum_{ijhkab} i\int d^4x \frac{d^4x'}{\hbar} \tilde{\Lambda}^{ab}_{ijhk}(x,x')\left(\hbar \tilde{Q}^{ab}_{ijhk} - v^a_{ij}(x)v^b_{hk}(x')\right) \tag{14}$$

As the disorder average restores translational and rotational invariance, the mean field approximation has to reflect these symmetries. In addition we assume replica diagonal pair modes:

$$\tilde{Q}^{ab}_{ijlm}(x,x') = \delta_{ab}\left(\delta_{il}\delta_{jm} + \delta_{im}\delta_{jl}\right)\chi_2(x-x') \tag{15}$$

$$\tilde{\Lambda}^{ab}_{ijlm}(x,x') = i\delta_{ab}\left(\delta_{il}\delta_{jm} + \delta_{im}\delta_{jl}\right)\Sigma_2(x-x') \tag{16}$$

$$Q^{ab}_{ijlm}(x,x') = \delta_{ab}\left(\delta_{il}\delta_{jm} + \delta_{im}\delta_{jl}\right)\chi_1(x-x') \tag{17}$$

$$\Lambda^{ab}_{ijlm}(x,x') = i\delta_{ab}\left(\delta_{il}\delta_{jm} + \delta_{im}\delta_{jl}\right)\Sigma_1(x-x') \tag{18}$$

This ansatz removes the bare anharmonic interaction terms with μ_0 and Λ from the effective action in agreement with the previous scalar approach [13], and in addition the last term of Eq. (12).

We kept $\hbar$ explicitly for identifying the quantum contributions: the phonon dynamics are governed by the effective Lagrange density

$$\begin{aligned}\mathcal{L}_{eff} &= u^{(1)}_{ij}(x)G^{-1}_{0ijlm}(x-x')u^{(1)}_{lm}(x') \\ &\quad - u^{(1)}_{ij}(x)i\Lambda^{(1)}_{ijlm}(x-x')u^{(1)}_{lm}(x') \\ &\quad - v^{(1)}_{ij}(x)i\tilde{\Lambda}_{ijlm}(x-x')v^{(1)}_{lm}(x')\end{aligned} \tag{19}$$

in which the Lagrange multipliers $\Lambda, \tilde{\Lambda}$ enter as external fields. As far as their dynamics are independent of $\hbar$, we are just left with a classical continuum field theory, subjected to canonical statistics. This happens in the case of zero anharmonicity, in which the problem is reduced to the determination of the classical spectral function [5,8].

Proceeding with the mean field approach, a Matsubara decomposition of the euclidean action (12) is done with the following conventions:

$$\mathbf{u}_i(\mathbf{x},\tau) = \frac{1}{\sqrt{\beta V}}\sum_{n,\mathbf{k}} u_i(\omega_n,\mathbf{k})e^{i\omega_n\tau - i\mathbf{k}\cdot\mathrm{x}} \tag{20}$$

$$Q(x-x') = \frac{1}{\beta V}\sum_k Q(k)e^{i(k,x-x')} \tag{21}$$

Here we introduced the four-vector notation $k = (\mathbf{k},\omega_n)$, $(k,x) = i\omega_n\tau - i\mathbf{k}\cdot\mathbf{x}$. The imaginary time displacement field is integrated out leaving the effective action in terms of the composite fields.

Minimizing this effective action yields the saddle-point equations satisfied by the composite fields (22–25). Linearizing these equations leaves just the classical harmonic theory [5,7,8], in which the self energy satisfies the self consistent Born approximation. Therefore they establish a reasonable generalization of the harmonic theory.

$$\Sigma_1(\mathbf{q},\omega_n) = \frac{1}{V}\sum_{\mathbf{k}} \mathrm{K}_\mu(\mathbf{k}-\mathbf{q})(\chi_L(\mathbf{k},\omega_n) + \chi_T(\mathbf{k},\omega_n)) + \frac{\Sigma^L_{an}(\mathbf{q},\omega_n)}{2} \tag{22}$$

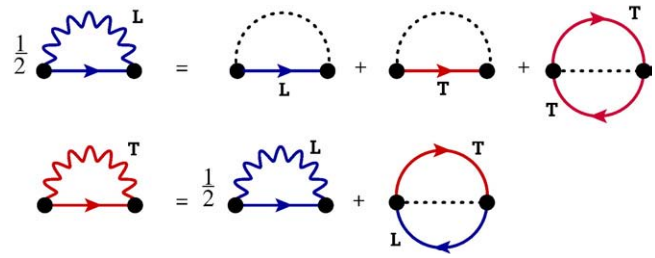

Fig. 2. Diagrammatic representation of the anharmonic mean field equations: blue = L, red = T; full lines are susceptibilities, dashed lines represent the correlation function; winding lines are the full self energies. (For interpretation of the references to colour in this figure legend, the reader is referred to the web version of this article.)

$$\begin{aligned}\Sigma_2(\mathbf{q},\omega_n) &= -\frac{\hbar}{6\beta V^2}\sum_{\mathbf{k},\mathbf{p},\omega_m}(\chi^*_T(\mathbf{p}+\mathbf{q},\omega_n-\omega_m) \\ &\quad + \chi^*_L(\mathbf{p}+\mathbf{q},\omega_n-\omega_m))K_\mu(\mathbf{p}-\mathbf{k})\chi_T(\mathbf{k},\omega_m) \\ &= \frac{1}{2}\Sigma^L_{an}(\mathbf{q},\omega_n) + \Sigma^T_{an}(\mathbf{q},\omega_n) \\ &= -\frac{\hbar}{6\beta V}\sum_{\mathbf{k}}\left(\Sigma_1(\mathbf{k}+\mathbf{q},\omega_{n-m}) - \frac{\Sigma^L_{an}(\mathbf{k}+\mathbf{q},\omega_{n-m})}{2}\right)\chi_T(\mathbf{k},\omega_m)\end{aligned} \tag{23}$$

$$\chi_L(\mathbf{q},\omega_m) = \frac{\mathbf{q}^2}{\rho\omega_n^2 + \mathbf{q}^2(\lambda + 2\mu_0 - 2\Sigma_1(\mathbf{q},\omega_n))} = \mathbf{q}^2 G_L(\mathbf{q},\omega_m) \tag{24}$$

$$\chi_T(\mathbf{q},\omega_m) = \frac{\mathbf{q}^2}{\rho\omega_n^2 + \mathbf{q}^2(\mu_0 - \Sigma_1(\mathbf{q},\omega_n) - \Sigma_2(\mathbf{q},\omega_n))} = \mathbf{q}^2 G_T(\mathbf{q},\omega_m) \tag{25}$$

The quadratic (in χ) terms emerge from the disorder enhanced anharmonic interaction, all anharmonic terms vanish in the case of zero disorder $K_\mu \to 0$.

These saddle-point equations can be represented diagrammatically (Fig. 2). Indeed, they resemble the structure of a calculation of the self energy to first order in the anharmonic and disorder-induced interaction. In the following we exploit this analogy for justifying the most obvious approximation to Eqs. (22–25), the *mode-decay approximation*.

2.4. Mode-decay approximation

We choose an exponential correlation function $K_\mu((\mathbf{x}-\mathbf{x}')) = \Delta^2\exp\left(-\frac{|(\mathbf{x}-\mathbf{x}')|}{\xi}\right)$, with Δ^2 the variance of the shear modulus and ξ the correlation length. The small anharmonic corrections to the longitudinal phonon propagator are estimated by expanding Eqs.(22–25) around the solution of the linearized saddle-point equations:

$$\chi_i = \overline{\chi}_i + \delta\chi_i \tag{26}$$

$$\Sigma_i = \overline{\Sigma}_i + \delta\Sigma_i \tag{27}$$

The lowest order anharmonic correction to the longitudinal phonon self energy is represented through the last diagram of Fig. 2, but with the full susceptibilities replaced by the disorder-dressed ones $\overline{\chi}_i$:

$$\delta\Sigma_L(\mathbf{q}\to 0,\omega_n) = -\frac{\hbar}{6\beta V^2}\sum_{\mathbf{k},\mathbf{p},\omega_m}\overline{\chi}_T(\mathbf{p},\omega_n-\omega_m)K_\mu(\mathbf{p}-\mathbf{k})\overline{\chi}_T(\mathbf{k},\omega_m) \tag{28}$$

Please cite this article as: C. Tomaras, et al., Replica field theory for anharmonic sound attenuation in glasses, J. Non-Cryst. Solids (2010), doi:10.1016/j.jnoncrysol.2010.05.084

Eq. (28) is recasted by the Matsubara technique [29]:

$$\delta\Sigma_L(\mathbf{q}\to 0,\omega_n) = -\frac{\hbar}{12V^2\pi}\sum_{\mathbf{k},\mathbf{p}}\int_{-\infty}^{\infty} d\omega \coth\left(\frac{\beta\omega}{2}\right) \times \overline{\chi}_T(\mathbf{p},\omega_n - i\omega_+)K_\mu(\mathbf{p}-\mathbf{k})\overline{\chi}_T''(\mathbf{k},i\omega_+) \tag{29}$$

$$= -\frac{\hbar}{6V^2\pi}\sum_{\mathbf{k},\mathbf{p}}\int_0^{\infty} d\omega \coth\left(\frac{\beta\omega}{2}\right)\overline{\chi}_T''(\mathbf{k},i\omega_+) \tag{30}$$

$$\times K_\mu(\mathbf{p}-\mathbf{k})(\overline{\chi}_T(\mathbf{p},\omega_n - i\omega) - \overline{\chi}_T(\mathbf{p},\omega_n + i\omega))$$

$$\approx -\frac{\hbar\Delta^2\xi^3}{6\pi^4}\int_0^{\infty} d\omega \int_0^{k_D} dk k^2 \int_0^{k_D} dp p^2 \coth\left(\frac{\beta\omega}{2}\right) \tag{31}$$

$$\times (\overline{\chi}_T(\mathbf{p},\omega_n - i\omega) - \overline{\chi}_T(\mathbf{p},\omega_n + i\omega))\overline{\chi}_T''(\mathbf{k},i\omega_+)$$

The Fourier transformed density-correlation function is linked to the dynamical longitudinal susceptibility, via the fluctuation–dissipation theorem:

$$\langle\rho^*(\mathbf{k},\omega)\rho(\mathbf{k},\omega)\rangle = \frac{1}{\pi}\coth\left(\frac{\beta\omega}{2}\right)\chi_L''(\mathbf{k},\omega_n = i\omega_+) = \frac{1}{\pi}\coth\left(\frac{\beta\omega}{2}\right)\chi_L''(k,\omega_+) \tag{32}$$

The Brillouin linewidth is then just the width of the longitudinal susceptibility at resonance

$$\Gamma(k) = k\Sigma_L''(\omega k)\,/\,v_L \quad \omega_k = v_L k. \tag{33}$$

At room temperature, the anharmonic contribution to the imaginary part of the self energy reads

$$\delta\Sigma_L''(\omega_n = i\Omega_+) = \frac{\Delta^2 k_B T\xi^3}{3\pi^4}\int_{(k,p,\omega)}\frac{k^2p^2}{\omega}\,\overline{\chi}_T''(\mathbf{k},\omega_+) \times\left(\overline{\chi}_T''(\mathbf{p},\omega_+ + \Omega) - \overline{\chi}_T''(\mathbf{p},\omega_+ - \Omega)\right). \tag{34}$$

The transverse susceptibility

$$\chi_T''(\mathbf{k},\omega_+) = \frac{1}{\rho v_T^2}\frac{\mathbf{k}^2\Sigma''(\omega_+)}{(-\omega_+^2 + v_T^2\mathbf{k}^2)^2 + \mathbf{k}^4\left(\Sigma''(\omega_+)\right)^2} \tag{35}$$

consists not only of a Brillouin-peak, but resembles the shape of the self energy in self consistent Born approximation (Fig. 3).

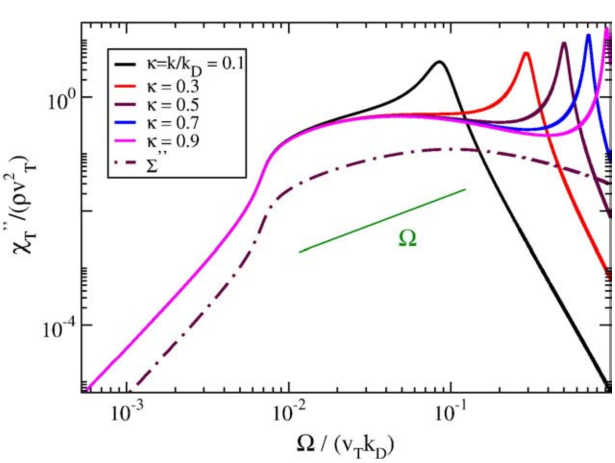

Fig. 3. The spectral density function $\chi_T''(\mathbf{k},\omega_+)$ for various wave numbers.

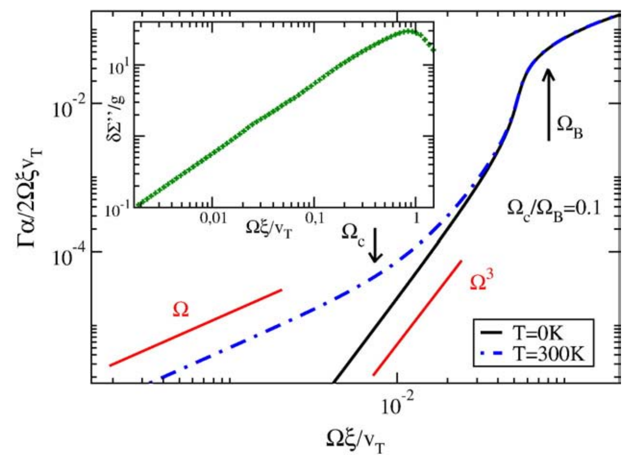

Fig. 4. Full Brillouin linewidth due to disorder and anharmonicity for $(v_L/v_T)^2=2.52$, $\Delta^2=0.99, \Delta_c^2=0.401\rho^2 v_T^4, \xi=2/k_D$ and $T=300K$ inset: the anharmonic self energy integral (35) divided by the anharmonicity parameter $g=\Delta^2 k_B T/(3\pi^4\xi^3\rho^3 v_T^4)$.

For numerical evaluation we introduce dimensionless quantities, $\tilde{\omega} = \frac{\omega\xi}{v_T}, \tilde{k} = k\xi, \tilde{\chi}'' = \chi''\rho v_T^2$.

$$\delta\Sigma_L''\left(\tilde{\Omega}_+\right) = \frac{\Delta^2 k_B T}{3\pi^4\xi^3\rho^3 v_T^4}\int_0^{k_D\xi} d\tilde{k}\tilde{k}^2\int_0^{k_D\xi} d\tilde{p}\tilde{p}^2\int_0^{\infty} \times \frac{d\tilde{\omega}}{\tilde{\omega}}\left(\tilde{\chi}_T''(\tilde{\mathbf{p}},\tilde{\omega}_+ + \tilde{\Omega}) - \tilde{\chi}_T''(\tilde{\mathbf{p}},\tilde{\omega}_+ - \tilde{\Omega})\right)\tilde{\chi}_T''\left(\tilde{k},\tilde{\omega}_+\right) \tag{36}$$

The sound-attenuation function exhibits a linear behavior at frequencies below the boson peak and drops off above (see the inset of Fig. 4). This happens because the main contribution to the integral (36), for frequencies below the boson peak, comes from the band of irregular delocalized high-frequency modes; these states contribute a wide $\chi_T''\propto\omega$ regime, situated above the boson peak, to the disordered spectral density (see Fig. 3), for which the kernel $\tilde{\chi}_T''\left(\tilde{\mathbf{p}},\tilde{\omega}_+ + \tilde{\Omega}\right) - \tilde{\chi}_T''\left(\tilde{\mathbf{p}},\tilde{\omega}_+ - \tilde{\Omega}\right)$ can be replaced with $\tilde{\Omega}\partial\tilde{\omega}\tilde{\chi}_T''(\tilde{\mathbf{p}},\tilde{\omega}_+)$.

2.5. Estimation of the crossover frequency in SiO²

We estimate the amount of the attenuation induced by anharmonicity as compared with the disorder-induced one. The ratio $R(\Omega) = \Gamma_{an}(\Omega)\,/\,\Gamma_{dis}(\Omega)\propto\delta\Sigma_L\left(\tilde{\Omega}\right)/\,\tilde{\Omega}$, which becomes frequency-independent beyond the boson peak, determines the crossover frequency. This ratio is fixed by the parameters Δ^2 and ξ, which set up the boson peak position, and the temperature. For example SiO_2 requires $\Delta^2=0.99\Delta_c^2=0.401\rho^2 v_T^4$ and $\xi=2/k_D$. The ratio of the squared sound velocities is $(v_L/v_T)^2=2.52$ and the Debye cutoff 1.6×10^{10}/m [6]. At room temperature $k_B T k_D^3/\rho v_T^2=0.6$ we obtain $\delta\Sigma_L''\left(\tilde{\Omega}\right)\approx 0.0045\,\tilde{\Omega}$, i.e. $T_0=7.3\cdot 10^5 K$. Fig. 4 shows the full Brillouin linewidth due to disorder and anharmonicity. The anharmonic corrections already lead to deviations from the disordered contribution slightly below the shoulder of the boson peak, the highest frequency, where the Akhiezer-like behavior is present in SiO_2 is therefore predicted to be one order of magnitude below the boson peak, i.e. in the 100 GHz regime. In general, for observing the Rayleigh-law one needs to go to low enough temperature, which shifts the crossover towards lower frequencies.

Let us now discuss the possible role of potential-induced anharmonicity. There is no problem to introduce interactions involving longitudinal and transverse Mode-Grüneisen parameters $g_{L,T}$ into the theory. In the longitudinal case one just has to replace Δ^2 by $(1+g_L^2)\Delta^2$ in the saddle-point Eqs. (22–25). This will shift the crossover from Akhiezer-like to Rayleigh scattering upwards and reduce the "Rayleigh window" between the Akhiezer–Rayleigh crossover and the boson peak. Within our continuum description, it is not possible to judge the importance of the Mode-Grüneisen parameters $g_{L,T}$, because they are effective constants which have to be calculated from a certain lattice theory, taking into account the microscopic details of the interaction. It has been pointed out by Fabian et al. [17], that the Grüneisen parameters which they have extracted from their simulations are unusually strong, with respect to the bare crystalline couplings. However, a suitable choice of the parameters for the Stillinger–Weber potential [30] used in their simulations [18] should account for the non-linear part of the strain tensor as well. Hence their strong Grüneisen parameters γ_i, should not be confused with our non-linear couplings $g_{L,T}$, which may as a first guess be identified with their rather weak crystalline counterparts [25], as long as one deals with weak disorder. However it cannot be excluded, that strong disorder or impurities drive these constants to a strong coupling regime, in a renormalization group approach. Therefore, it has to be determined by experiment, whether our "minimal" description is sufficient, or one has to deal with Grüneisen parameters.

The SiO_2 measurement, performed by Masciovecchio et al. [20], exhibits the Akhiezer–Rayleigh crossover around 100 GHz, which fits our estimates quite well. In contradiction Devos et al. [21] claim the crossover to take place at 400 GHz, however they performed their measurements on vitreous SiO_2, which shelters several defects. It is at the heart of impurity physics, that defects give rise to additional interactions, e.g. anharmonicities. This can lead to enhanced Mode-Grüneisen parameters $g_{L,T}$, which then have to be taken into account. In several experiments dealing with vibrational spectra near and below the glass transition [31,32] one observes an increase of the DOS in the boson peak regime. Within the mode-decay approximation one can account for the trends but not numerically reproduce such spectra. We believe that one has to solve the full mode-coupling Eqs. (22–25) in order to be able to do so.

3. Conclusion

In conclusion we developed a consistent perturbative treatment of the anharmonic contribution to the Brillouin linewidth in disordered solids. Our treatment solely in terms of elasticity parameters, which enter into the mean values and correlation functions suggests a correlation between the boson peak position and the Akhiezer–Rayleigh crossover at temperatures scaled with the Debye temperature. Further developments in experimental techniques are required to explore this extremely interesting frequency window in the upper GHz regime.

Acknowledgement

We are grateful to G. Ruocco for many helpful discussions and hospitality at Universität "La Sapienza," Rome. C.T. is grateful to K. Binder and R. Schilling for hospitality at University Mainz. Financial support by the Excellence Cluster "Nanosystems Initiative Munich 'NIM'" is gratefully acknowledged.

References

[1] W. Schirmacher, G. Diezemann, C. Ganter, Phys. Rev. Lett. 81 (1998) 136.
[2] W. Schirmacher, M. Wagener, in: D. Richter, A.J. Dianoux, W. Petry, J. Teixeira (Eds.), Dynamics of Disordered Materials, Springer-Verlag Heidelberg, 1989, p. 231.
[3] W. Schirmacher, M. Wagener, Philos. Mag. B 65 (1992) 607.
[4] E. Maurer, W. Schirmacher, J. Low Temp. Phys. 137 (2004) 453.
[5] W. Schirmacher, Europhys. Lett. 73 (2006) 892.
[6] W. Schirmacher, G. Ruocco, T. Scopigno, Phys. Rev. Lett. 98 (2007) 025501.
[7] W. Schirmacher, B. Schmid, C. Tomaras, G. Viliani, G. Baldi, G. Ruocco, T. Scopigno, Phys. Status Solidi C 5 (2008) 862.
[8] B. Schmid, W. Schirmacher, Phys. Rev. Lett. 100 (2008) 137402.
[9] V. Martin-Mayor, G. Parisi, P. Verroccio, Phys. Rev. E 62 (2000) 2373.
[10] T.S. Grigera, V. Martin-Mayor, G. Parisi, P. Verroccio, Phys. Rev. Lett. 87 (2001) 085502.
[11] R. Kühn, U. Horstmann, Phys. Rev. Lett. 78 (1997) 4067.
[12] J.W. Kantelhardt, S. Russ, A. Bunde, Phys. Rev. B 63 (2001) 064302.
[13] E. Maurer, W. Schirmacher, M. Poehlmann, Phys. Status Solidi B 230 (2002) 31.
[14] D. Belitz, T. Kirkpatrick, Rev. Mod. Phys. 66 (1994) 261.
[15] D. Belitz, T. Kirkpatrick, Phys. Rev. B 56 (1997) 6513.
[16] M. Stone, A.J. McKane, Ann. Phys. 131 (1981) 36 (New York).
[17] J. Fabian, P.B. Allen, Phys. Rev. Lett. 82 (1999) 1478.
[18] J.L. Feldman, M.D. Kluge, P.B. Allen, F. Wooten, Phys. Rev. B 48 (1993) 12589.
[19] J. Hasson, A. Many, Phys. Rev. Lett. 35 (1975) 792.
[20] C. Masciovecchio, G. Baldi, S. Caponi, L. Comez, S. Di Fonzo, D. Fioretto, A. Fontana, A. Gessini, S.C. Santucci, F. Sette, G. Viliani, P. Vilmercati, G. Ruocco, Phys. Rev. Lett. 97 (3) (2006) 035501.
[21] A. Devos, M. Foret, S. Ayrinhac, P. Emery, B. Rufflé, Phys. Rev. B 77 (10) (2008) 100201.
[22] A. Akhiezer, J. Phys. 1 (1939) 277 (Moscow).
[23] L. Landau, E. Lifshitz, Theory of Elasticity, Pergamon Press, New York, 1991.
[24] P.M. Chaikin, T.C. Lubensky, Principles of Condensed-Matter Physics, Cambridge University Press, New York, 1995.
[25] R. Cowley, Rep. Prog. Phys. 31 (1968) 123.
[26] G. Rumer, L. Landau, Phys. Z. Sowj. 11 (1936) 18.
[27] V.N. Popov, Functional Integrals in Quantum Field Theory and Statistical Physics, D.Reidel Publishing Company, Dordrecht, 1983.
[28] V.N. Popov, L.D. Fadeev, Sov. Phys. Usp. 16 (1974) 777.
[29] A.L. Fetter, J.D. Walecka, Quantum Theory of Many-particle Systems, Dover Publications, Mineola, New York, 2003.
[30] F.H. Stillinger, T.A. Weber, Phys. Rev. B 31 (1985) 5262.
[31] W. Petry, J. Wuttke, Phys. Rev. E 52 (1995) 4026.
[32] A.I. Chumakov, I. Sergueev, U. van Bürck, W. Schirmacher, T. Asthalter, R. Rüffer, O. Leupold, W. Petry, Phys. Rev. Lett. 92 (2004) 245508.